

Supplementary material to AICC2012 Common for Bazin et al. (2013) and Veres et al. (2013)

The method for the building of AICC2012 is an improved version of Datice presented in Lemieux-Dudon et al. (2010), hereafter LD2010, for 4 ice cores (Vostok, EPICA Dome C, EPICA Dronning Maud Land, NorthGRIP) and modified for TALDICE by Buiron et al. (2011). The aim is to combine chronological information from data and model to build coherent and precise timescales with associated estimates of uncertainty range. For this, the Datice tool needs several inputs. First, independent background scenarios for thinning, accumulation rate and lock-in depth in ice equivalent (LIDIE) have to be implemented for each of the 5 ice cores. Then, Datice builds a correction function associated with each scenario (thinning, accumulation rate, LIDIE). The correction function is more or less allowed to modify the initial scenario depending on the variance associated with each scenario for each ice core. The variance scenarios need to be prescribed by the user. Then, Datice incorporates markers from ice core records such as absolute or orbital age markers on each ice core, gas and ice stratigraphic links between the ice cores and constraints for Δ depth (depth difference between the signatures of the same event in the ice and gas phases). The error statistics of the background and observations must be decorrelated for a proper application of the Datice inverse method.

An important aspect of the Datice initialisation that was not modified in this study from LD2010 is the correlation length that imposes the depth range of the ice core on which a marker influences the correction function. If the correlation length is large, a marker has the effect of modifying on a large depth range the correction function. Finally, Datice calculates a cost function that measures the distance between background scenarios and new scenarios as well as between new scenarios and data constraints. A too high cost function obviously means that there are incoherencies between the inputs proposed by the user.

In the previous studies, the dating method was optimized for the last 50 ka and here we have extended it over the past 800 ka. Several improvements have been made compared to the study of Lemieux-Dudon et al. (2010), both in some background scenarios and in the parameterization of the variance associated with these scenarios. In addition, our new chronology also incorporates numerous new stratigraphic, absolute and orbital markers that strongly reduce the dating uncertainty especially for the last glacial cycle. We provide below all the necessary information and input parameters to run

the open source Datice tool and obtain the AICC2012 chronology for NorthGRIP, Vostok, EDC, EDML and TALDICE. When nothing is specified (i.e. correlation length), then the original LD2010
30 parameterization is still used.

1 Background parameters

For each ice core, 3 background parameters are needed: accumulation rate, thinning, LIDIE.

1.1 Accumulation rate

For all Antarctic ice cores, we have followed the classical estimate of accumulation rate based on an
35 exponential relationship between accumulation rate and water isotopes (as temperature proxies). For the 4 Antarctic cores, we have thus used exactly the same accumulation rate scenarios as those pre-scribed in Lemieux-Dudon et al. (2010) and Buiron et al. (2011) (for TALDICE). Note that for Vostok and TALDICE, changes in elevation are taken into account to correct the temperature estimate from the water isotopic profiles. With regard to GICC05, in order to constrain AICC2012 to match
40 GICC05 for the past 60 ka, we have deduced the accumulation rate from the annual layer thickness given by the GICC05modelext (Vinther et al., 2006; Rasmussen et al., 2006; Andersen et al., 2006; Svensson et al., 2008; Wolff et al., 2010) and the strain rate given by the Dansgaard-Johnsen model tuned for NorthGRIP (NorthGRIP Community Members, 2004; Andersen et al., 2006).

1.2 Thinning

45 For Vostok and EDC, we used the same thinning function as in LD2010. For Vostok, the thinning function is deduced from the accumulation and FGT1 age scale. For EDC, it is deduced from the accumulation and the EDC3 model age scale. Concerning EDML, the thinning function is obtained from the flow model of Huybrechts et al. (2007). Such a background thinning function is different from the one implemented in Lemieux-Dudon et al. (2010) and especially avoids spurious peaks
50 around 500 m depth. We used the same thinning function as Buiron et al. (2011) for TALDICE, obtained from a 1D flow model. For NGRIP, the strain rate is given by the Dansgaard-Johnsen model tuned for NorthGRIP (NorthGRIP Community Members, 2004; Andersen et al., 2006) and used here as thinning background scenario. Note that the background thinning function for NorthGRIP used in
55 Lemieux-Dudon et al. (2010) was not fully consistent with GICC05. As a consequence, there was a slight disagreement between the LD2010 NorthGRIP timescale and GICC05 at the rapid warmings associated with Dansgaard-Oeschger events with differences of ± 30 a. These differences do not exist anymore for AICC2012 (Fig. 5).

We performed a test of the influence of different thinning functions as input for Vostok (the one used to build AICC2012 and a "test thinning function"). The test thinning function is very simplified
60 and obtained using IceChronoModel (F. Parrenin Pers. comm.). We can see that the thinning outputs

with Datice tend to the same behaviour. The resulting chronology is not significantly changed with the test thinning function as input (Fig. 1).

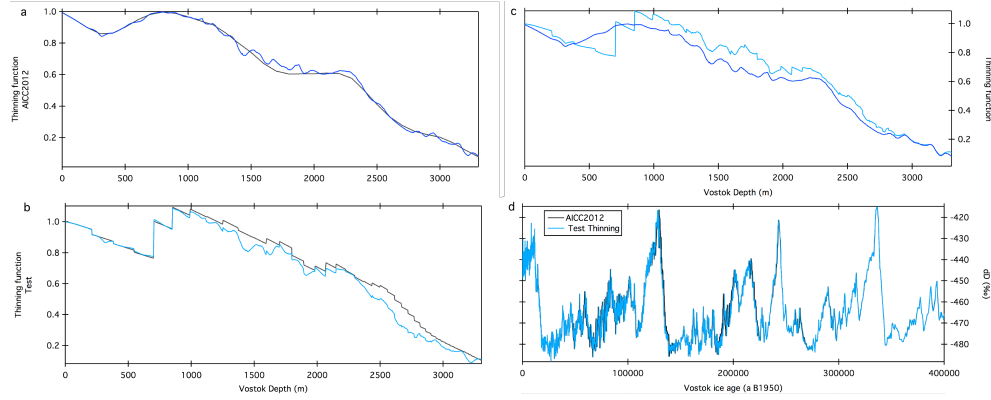


Fig. 1. Thinning function tests on Vostok. Grey curves are background and blue curves are Datice results. a: thinning function as in AICC2012. b: test thinning function. c: comparison of Datice outputs (AICC2012 in dark blue, test thinning function in light blue). d: comparison of the resulting chronologies.

1.3 LIDIE

Initially, the background LIDIE for each site came from the Goujon et al. (2003) firnification model (Lemieux-Dudon et al., 2010). The model has been validated over NorthGRIP (Landais et al., 2004; Huber et al., 2006; Guillevic et al., 2013) but seems to overestimate LIDIE for glacial conditions in Antarctic sites except for TALDICE (Landais et al., 2006; Parrenin et al., 2012a; Capron et al., 2013). Parrenin et al. (2012a) have suggested that $\delta^{15}\text{N}$ may provide more realistic constraints on past LID even in low accumulation rate sites. We have thus performed tests with Datice comparing the output LIDIE when using as input the firnification model (background scenario LIDIE 1) and a LIDIE inspired by the $\delta^{15}\text{N}$ profile on each site except NorthGRIP (background scenario LIDIE 2). For this scenario 2, we have assumed that the convective zone did not change over time and took a 0 m convective zone for EDML, TALDICE and EDC and 13 m for Vostok as observed on present firn (Landais et al., 2006). The LIDIE can then be calculated from the $\delta^{15}\text{N}$ variations in the absence of any rapid temperature variation (2°C in 100 a) at the surface. This condition is valid in Antarctica over the considered period.

$$\text{LIDIE} = 0.7 \cdot \delta^{15}\text{N} \cdot R \cdot T / g$$

where T is the mean firn temperature, R the ideal gas constant and g the standard gravity. The factor 65 0.7 stands for the mean density of the firn. A small correction for temperature gradient in the firn affects the glacial LIDIE in low accumulation rate sites like Vostok and Dome C by 3 m at maximum. This correction has been taken into account using the firn gradient calculated by the Goujon

et al. (2003) model. For building scenario 2, we have used $\delta^{15}\text{N}$ profiles when they were available (Dreyfus et al. (2010) for EDC, Sowers et al. (1992) for Vostok, Capron et al. (2013) for TALDICE and EDML). None of these profiles cover the whole depth of the 4 Antarctic ice cores. We then take advantage of the strong link between $\delta^{15}\text{N}$ and δD evolution on an age scale (Dreyfus et al., 2010). As a consequence, we could build the missing part of the $\delta^{15}\text{N}$ profiles from the $\delta\text{D} - \delta^{15}\text{N}$ regression over Terminations using the official ice and gas timescales for each core. Such method has been applied to fill the gaps of the $\delta^{15}\text{N}$ profiles for EDC over the last 300 ka (except for Terminations where $\delta^{15}\text{N}$ profiles are available, Dreyfus et al. (2010)). For TALDICE, the firnification model has been shown to be in good agreement with $\delta^{15}\text{N}$ data over the last deglaciation (Capron et al., 2013) so that we have used the Goujon et al. (2003) LIDIE output to fill the gap over the last interglacial and last glacial periods.

The different background scenarios for LIDIE have a small impact on the final chronology because the variance associated with the LIDIE background scenario is quite large. As a consequence, the Antarctic output LIDIE are mostly constrained by the ice and gas stratigraphic points, especially over the last glacial period where many stratigraphic tie-points are available (see corresponding section below). During the last glacial period at EDC, the agreement is better between output and background LIDIE when scenario LIDIE 2 is used (Fig. 2) especially over Termination I. There are several reasons why we do not end with the same LIDIE after analyses at Dome C in LD2010 and in AICC2012. The first reason, which is probably not the main one, is that we have much more stratigraphic points in AICC2012 than in LD2010. The second reason is linked to the background LIDIE scenarios. In AICC2012, the LIDIE background scenario of NorthGRIP is significantly lower than the one in LD2010 (Figure 5 of Veres et al. (2013)). This is due to a better constrained temperature input scenario for the firn densification model used to obtain the background LIDIE of NorthGRIP, in agreement with the full $\delta^{15}\text{N}$ record at NorthGRIP (Landais et al., 2004, 2005; Huber et al., 2006, P. Kindler, pers. comm.) which could not be used in LD2010. For this, we had to use a temporal relationship, $\alpha \sim 0.38$, to link the temperature variations to the ice $\delta^{18}\text{O}$ variations. Similarly, the EDML LIDIE background scenario is reduced in AICC2012 (scenario LIDIE 2) compared to the one of LD2010 as it is based on $\delta^{15}\text{N}$ rather than on firnification model. Finally, AICC2012 also incorporates TALDICE background LIDIE scenario given by the firnification model in agreement with the $\delta^{15}\text{N}$ estimate. Then, the numerous gas and/or ice stratigraphic markers, the NorthGRIP, EDML and TALDICE LIDIE are reflected also in the analysed LIDIE for Dome C. As a consequence, if the LIDIE scenarios are smaller at EDML and NorthGRIP in AICC2012 than in LD2010, this will automatically lead to a smaller LIDIE at EDC.

Finally, it should be noted that the Datice model can be run with several interpolations from the background scenario, i.e. a fast mode with an interpolation of the background scenario every 2 or 3

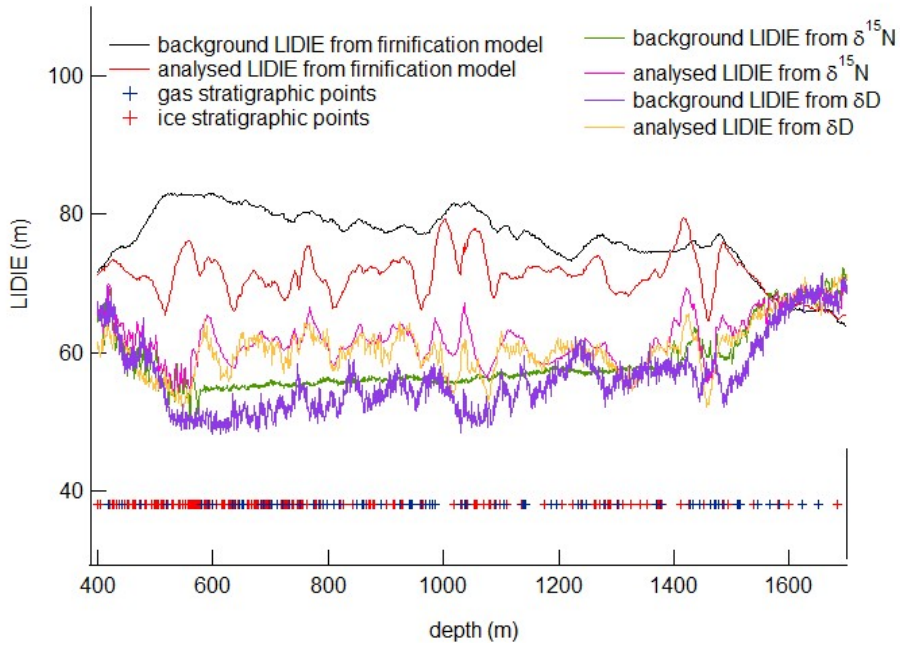


Fig. 2. Different tests on the EDC chronology for the choice of the best LIDIE scenario. Black line: LIDIE background scenario from the firnification model of Goujon et al. (2003). Red line: LIDIE output scenario when Datice is run with background LIDIE from the firnification model. Green line: LIDIE background scenario calculated from $\delta^{15}\text{N}$ values (Dreyfus et al. (2010) over TII; unpublished values for MIS 5). A linear interpolation has been applied between $\delta^{15}\text{N}$ based LIDIE at the beginning and at the end of the last glacial period to cover the period where no $\delta^{15}\text{N}$ measurements on EDC are available. Pink line: LIDIE output scenario when Datice is run with background LIDIE from $\delta^{15}\text{N}$ data. Purple line: LIDIE background scenario calculated from $\delta^{15}\text{N}-\delta D$ scenario. It has been observed that for different Antarctic sites, $\delta^{15}\text{N}$ and δD are well correlated on an age scale (Dreyfus et al., 2010; Capron et al., 2013). We use here the correlation between δD and $\delta^{15}\text{N}$ over the last Termination to obtain a synthetic $\delta^{15}\text{N}$ curve when $\delta^{15}\text{N}$ data are missing. Yellow line: LIDIE output scenario when Datice is run with background LIDIE from $\delta^{15}\text{N}-\delta D$ scenario.

Table 1. Origin of the background parameter profiles

| | Accu. | Thinning | LIDIE |
|---------|--------------|-------------------------------------|---|
| Vostok | From isotope | Accu. - FGT1 | $\delta^{15}\text{N}-\delta D$ |
| EDC | From isotope | Accu. - EDC3 model | $\delta^{15}\text{N}-\delta D$ |
| EDML | From isotope | Huybrechts et al. (2007) | $\delta^{15}\text{N}-\delta D$ |
| TALDICE | From isotope | 1D-flow model (Buiron et al., 2011) | $\delta^{15}\text{N}-\text{firn model}$ |
| NGRIP | From GICC05 | From GICC05 | Firn model |

105 points or a slow mode with use of the background scenario with its prescribed resolution (1 m for NorthGRIP, 0.55 m for EDC, 1 m from the surface down to 125 m and then 0.5 m below for EDML, 1 m for Vostok and 1 m for TALDICE). Since the initial resolution of the background scenario and the interpolation step may have an influence on the final chronology, we have performed tests with several resolutions. It appears that this effect is negligible compared to the effect of uncertainties
 110 associated with the tie-points or the variances associated with the background scenarios which are thus the important parameters to be imposed (see next section).

2 Variances profiles

Each background scenario is associated with a variance. If the variance is high, Datice is allowed to make a strong correction to the background scenario in the final chronology. On the opposite, if the
 115 variance is small, the final scenarios should be very close to the background ones.

We implemented variance profiles for accumulation rate, thinning function and LIDIE that have been slightly modified from their initial formulation in Lemieux-Dudon et al. (2010). They take into account the depth (variance increases with depth for some sites) as well as the deviation from the present-day conditions based on the accumulation rate values.

120 2.1 Thinning function

The variance on the thinning function is expressed as:

$$\sigma_T(z) = c_{T_1} + c_{T_2} \cdot \int^z \frac{D(z)}{T(z)} dz + c_{T_3} \cdot \frac{\sigma_{A,loc}}{\sigma_{A,loc}^{max}}$$

where c_{T_1} , c_{T_2} and c_{T_3} are user defined constant parameters (c_{T_2} equal $c \cdot 0.1/H$ where H is the maximum depth of the input and c a user defined constant), $T(z)$ is the thinning function, $D(z)$ the relative density, $\sigma_{A,loc}$ the local standard deviation of accumulation and $\sigma_{A,loc}^{max}$ the maximum standard deviation of accumulation. The last term was implemented in order to increase the thinning
 125 variances during transitions since it has been suggested that the mechanical properties of ice can be modified in these periods. The parameterization of this effect could be improved by modifying also the correlation length during these periods but would require additional tests for a correct parameterization. This last term is however of second order relatively to the depth dependence (Fig. 4b).

130 2.2 Accumulation rate

The variance is formulated as follows:

$$\sigma_A(z) = \sigma_{b,A} \cdot \frac{|A_0 - A|}{|A_0 - A|_{max}} \cdot \left(1 + c_{A_1} \frac{z}{z_{max}} \right)$$

with $\sigma_{b,A}$ being a reference standard deviation, A_0 is the mean Holocene accumulation rate, c_{A_1} is a constant parameter. The variance associated with the accumulation rate scenario thus increases

when the background accumulation rate strongly deviates from the Holocene value. The reason for such a parameterization is that the reconstruction of accumulation rate from water isotopes through the exponential law is semi-empirical and its extrapolation far from the present-day conditions may be problematic.

In order to avoid too small variances, a threshold value, σ_m , is implemented for each ice core. When σ_A is smaller than σ_m , then σ_A is recalculated as:

$$\sigma_A = \sigma_m \cdot \left(1 + c_{A_1} \frac{z}{z_{max}} \right)$$

where σ_m represents the minimum values, defined by user.

A dependence from upstream origin of the ice should be considered in the future.

2.3 LIDIE

The LIDIE variance is parameterized as:

$$\sigma_L(z) = \frac{\sigma_{b,L}}{\sigma_{b,A}} \cdot \frac{\sigma_A(z)}{1 + \frac{m_{A,loc}}{m_{A,loc}^{max}}}$$

135 with $m_{A,loc}$ being the local mean accumulation rate and $m_{A,loc}^{max}$ its maximum value over the length of the core, $\sigma_{b,L}$ is a reference standard deviation. In this case, the variance on the LIDIE increases with the variance on the accumulation rate, i.e. with the deviation from present-day conditions. This is justified by the fact that we do not have a standardized way to link LIDIE to accumulation rate or temperature (firnification model or $\delta^{15}\text{N}$ based estimate, see above).

140

An example of the resulting variances for the EDC core is presented on Fig. 3. The different coefficient values are given for each core in Table 2. The choice of variance remains necessary subjective but the following approach has been done:

- The depth dependence of the variances associated with accumulation rate and LIDIE has only been considered for sites located on a slope and not on a dome. Hence, c_{A_1} has been assigned a value of 1 for Vostok and EDML.
- A larger variance for LIDIE has been applied for sites where the firnification model and $\delta^{15}\text{N}$ approaches clearly disagree, i.e. for Vostok, EDML and EDC.
- A larger variance has been prescribed for EDML and Vostok thinning compared to EDC and NorthGRIP because their location on a slope make the estimate of the background thinning function from the glaciological model less certain.
- The thinning variance has been adjusted for TALDICE compared to EDC in order to avoid dating inconsistencies produced by the glaciological background scenario of TALDICE thinning.

Indeed, the background scenarios obtained from glaciological model for TALDICE gives an
 155 age model that is much too young with the δD optimum of MIS 5 occurring around 110 ka
 (Fig. 4a). This is in contradiction with available data suggesting that this optimum should
 occur around 130 ka (Waelbroeck et al., 2008), with an uncertainty of several ka. It is im-
 possible that Termination II was only 110 ka old. Using the initial variance for the thinning
 160 and accumulation rate of TALDICE produced a quite young Termination II because of the
 influence of the TALDICE background scenario on the final chronology. We therefore had to
 increase the variance associated with thinning at TALDICE (Fig. 4b).

- The variance on EDC and NorthGRIP thinning has been adjusted so that the new chronology
 of MIS 5 and MIS 4 lies between the EDC3 and NorthGRIPmodeext chronologies. These two
 initial chronologies where mostly derived from different glaciological constraints over this
 165 particular period and there is no reason why one chronology should be preferred compared to
 the other.

Table 2. Coefficient values of the variance profiles for the different ice cores. With respect to LD2010, c_{T_1} has
 been lowered, c_{T_2} has been adjusted for each ice core and the term c_{T_3} added. The values of σ_b for accumulation
 rate and LIDIE have been kept from LD2010 except the value of $\sigma_{b,A}$ which has been increased for EDML.

| | Thinning | | | Accu. rate | | LIDIE |
|---------|-----------|-----------|-----------|----------------|-----------|----------------|
| | c_{T_1} | c_{T_2} | c_{T_3} | $\sigma_{b,A}$ | c_{A_1} | $\sigma_{b,C}$ |
| Vostok | 0.01 | 0.000084 | 0.15 | 0.6 | 1 | 0.7 |
| EDC | 0.01 | 0.000030 | 0.15 | 0.7 | 0 | 0.7 |
| EDML | 0.01 | 0.000078 | 0.15 | 0.5 | 1 | 0.6 |
| TALDICE | 0.01 | 0.000268 | 0.15 | 0.6 | 0 | 0.6 |
| NGRIP | 0.01 | 0.000016 | 0.05 | 0.6 | 0 | 0.6 |

Many test of the variances assigned to the input scenarios were performed to evaluate the sensitivity of the final solution to initial model conditions but cannot be detailed here.

3 Observations

- 170 The different markers included in Datice are common for Veres et al. (2013) and Bazin et al. (2013).
 The database combines absolute ages, orbital markers, delta-depth markers and stratigraphic links
 in gas and ice phases to synchronize our five ice cores.
 The AICC2012 chronology is also constrained back to 800 ka with the use of orbital markers when
 absolute markers are missing (Bazin et al., 2013).
 175 Compared to the first Datice application used to produce the chronology delivered by Lemieux-
 Duodon et al. (2010), we wanted to suppress the climatic synchronization assumptions and avoid

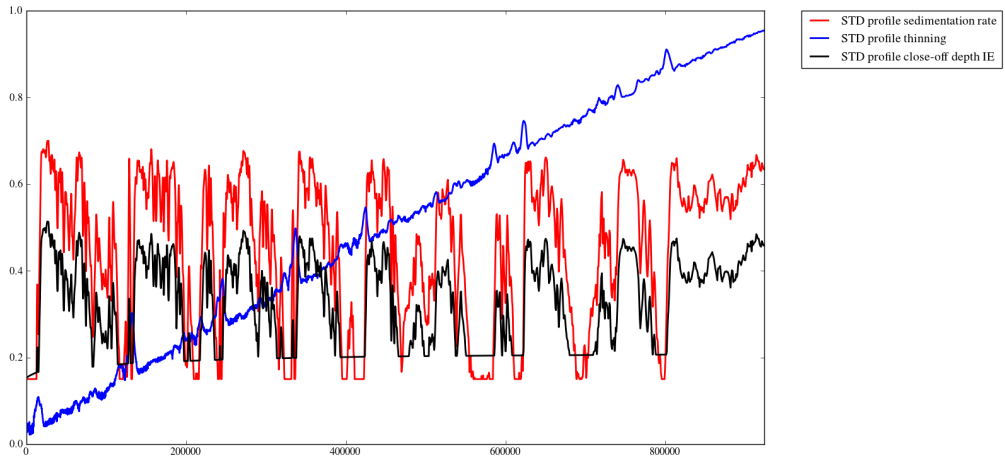


Fig. 3. Variances profiles of accumulation rate (red), LIDIE (black) and thinning function (blue) as function of age for EDC

circular synchronisation markers. We have thus removed or modified the following absolute markers:

- Climatic orbital markers derived from δD insolation matching at Vostok (Parrenin et al., 2001).
- Speleothem point at 130.1 ka - see main text of Bazin et al. (2013)
- Air content orbital markers at Vostok and EDC - they have been replaced by the new table of orbital markers as explained in Bazin et al. (2013).
- All points derived by successive transfer between the cores (Parrenin et al., 2007)

3.1 Absolute age markers

The absolute ages described here are obtained from independent dating of events recorded in the cores. All absolute ages have been determined by argon dating with the standard of Kuiper et al. (2008) (Fish Canyon sanidine at 28.201 ± 0.046 Ma). Ages of the Laschamp event, Mount Moulton eruption and Brunhes-Matuyama reversal have in some cases slightly changed from the published ages due to the re-calculation on the same standard.

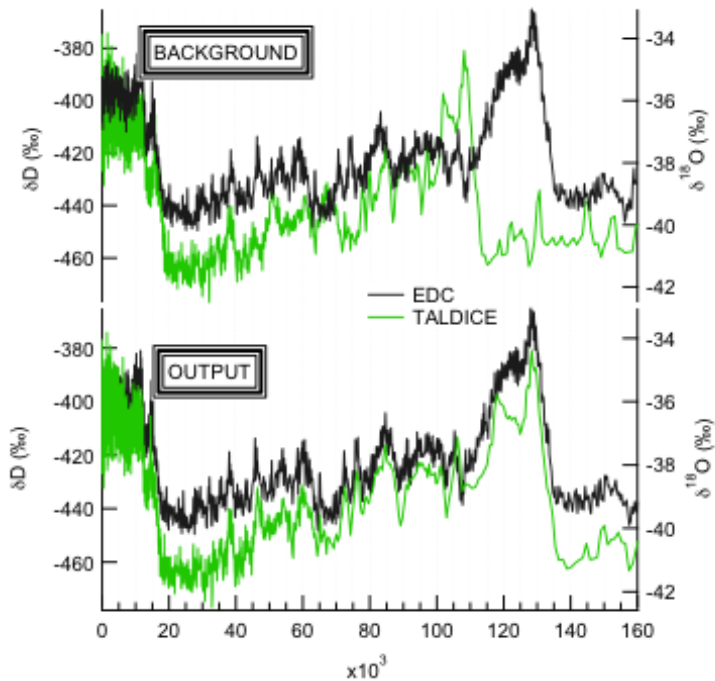


Fig. 4a. Upper panel: background chronologies from glaciological models for EDC (black) and TALDICE (green) Lower panel: output AICC2012 chronologies for EDC (black) and TALDICE (green)

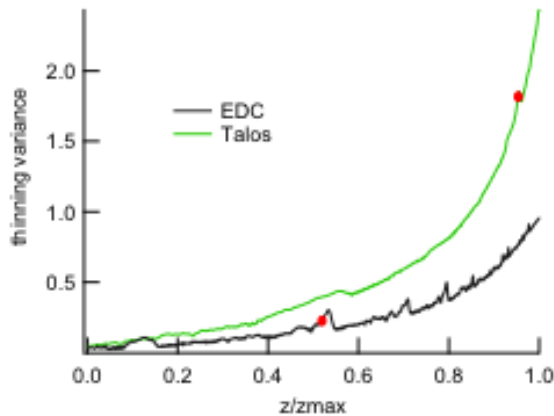


Fig. 4b. Thinning variances used for AICC2012 for EDC (black) and TALDICE (green). The red points correspond to the depth location of Termination II in the EDC and TALDICE ice cores.

190 3.1.1 Vostok

The absolute age markers for Vostok are deduced from ^{10}Be data. An age of 7.18 ± 0.10 ka at 178 m depth was assigned by comparison of the cosmogenic production of ^{10}Be and ^{14}C (Parrenin et al.,

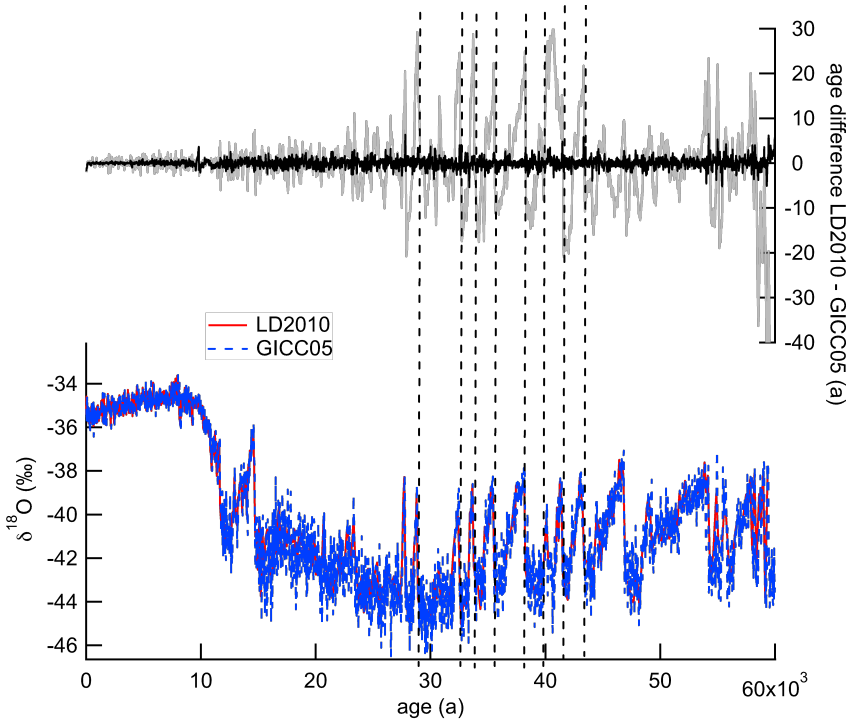


Fig. 5. NGRIP. Upper panel: difference between the LD2010 and GICC05 chronologies (grey); difference between the AICC2012 and GICC05 chronologies (black). Bottom panel: $\delta^{18}\text{O}$ records on the LD2010 and GICC05 chronologies.

2001; Raisbeck et al., 1998).

The second age marker corresponds to the Laschamp event recorded at 601 m, associated with a
195 revised age of 40.65 ± 0.95 ka (Raisbeck et al., 1987; Yiou et al., 1997; Singer et al., 2009).

3.1.2 EDC

EDC absolute ages are derived from ^{10}Be data and a tephra layer. The Laschamp event is recorded at 740 m and associated with an age of 40.65 ± 0.95 ka (Raisbeck et al., 2006; Singer et al., 2009). The Mount Moulton eruption tephra layer is observed at 1265.1 m (Narcisi et al., 2006). Its age
200 was first dated by Dunbar et al. (2008) on the Fish Canyon Tuff standard of Renne et al. (1998), and when converted to the Fish Canyon sanidine standard of Kuiper et al. (2008) we finally obtain an absolute age of 93.2 ± 4.4 ka. The last two ages are associated with the Brunhes-Matuyama (B-M) reversal and its precursor, observed at 3165.5 m and 3183.5 m, and dated at 780.3 ka and 798.3 ka respectively (Raisbeck et al., 2006; Dreyfus et al., 2008). We decided to enlarge the uncertainty
205 associated with these ages (from 3.5 to 10 ka) because many different ages of the B-M reversal are found in the literature spanning over ± 10 ka. These different ages can be explained by spatially

asynchronous changes in the field direction and smoothing effect of the signal due to lock-in depth uncertainties in marine sediments (Channell et al., 2010; Camps et al., 2011; Mochizuki et al., 2011; Dreyfus et al., 2008).

210 3.1.3 EDML

No absolute ages for the EDML ice core.

3.1.4 TALDICE

No absolute ages for the TALDICE ice core.

3.1.5 NGRIP

215 As in Lemieux-Dudon et al. (2010), we used absolute ages from GICC05 to force the model to respect the GICC05 chronology. Points were selected every 60 years over the last 60 ka (not listed, leading to 990 points). We associated an uncertainty of maximum 50 years with the purpose of constraining AICC2012 tightly to GICC05, but in return did not use the absolute gas age markers of table 6 of (Lemieux-Dudon et al., 2010). Note that the background parameters of NGRIP (deduced
220 from GICC05) and these markers are correlated, and this does not satify the hypothesis of independence between background and data. However, this is the only practical way to constrain the final timescale tightly to GICC05 for the last 60 ka (Fig. 5).

3.2 Orbital age markers

The choice of the orbital markers and associated uncertainties is fully explained in Bazin et al.
225 (2013). We will here only justify the keeping or removing of some orbital age markers presented in Bazin et al. (2013).

In the final version of AICC2012, we decided to remove three $\delta^{18}\text{O}_{\text{atm}}$ gas age markers around MIS 12 on the EDC ice core. Figure 6 shows a comparison of the background LIDIE (constructed from $\delta^{15}\text{N}$ measurements on EDC over this depth interval) and output LIDIE using $\delta^{18}\text{O}_{\text{atm}}$ and
230 $\delta\text{O}_2/\text{N}_2$ constraints. Clearly, the implementation of some $\delta^{18}\text{O}_{\text{atm}}$ markers creates spurious 10 m variations of the LIDIE during a period of 12 ka within MIS 12 and MIS 14. The background scenario for EDC LIDIE over these interglacial periods is based on $\delta^{15}\text{N}$ measurements. Because no convective zone is observed today at Dome C, we suppose that no convective zone should affect the relationship between $\delta^{15}\text{N}$ and LIDIE at this site over the past, so that the LIDIE estimate based on
235 $\delta^{15}\text{N}$ measurements is robust. These are the two reasons why we raised doubts on the coherency of these age markers. Still, removing these age markers had no significant impact on the final chronology within the uncertainty range (Fig. 6 bottom).

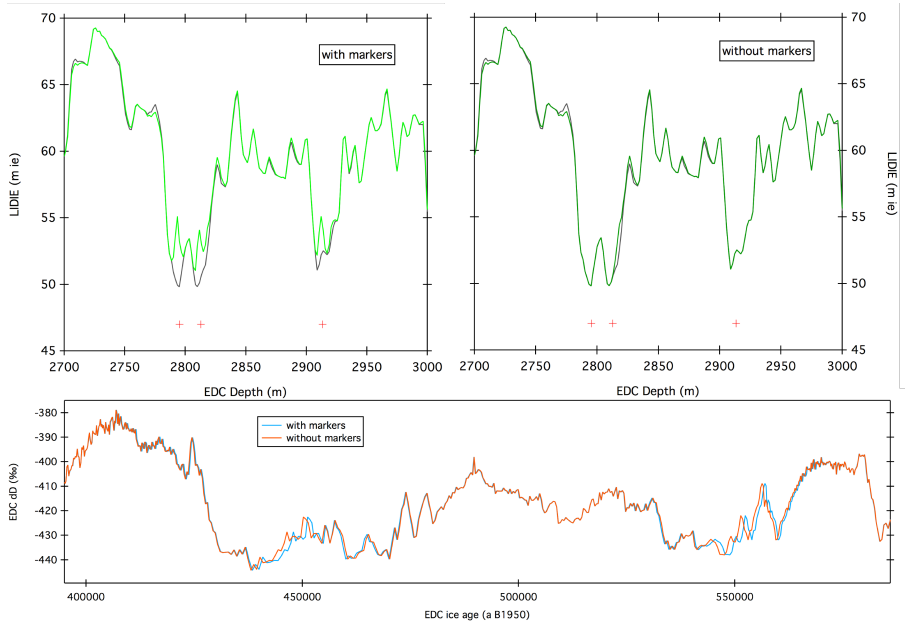


Fig. 6. Top: influence of $\delta^{18}\text{O}_{\text{atm}}$ markers on the LIDIE parameter at EDC around MIS 12. Red crosses mark position of the $\delta^{18}\text{O}_{\text{atm}}$ age markers that are included (left) or not (right) in our sensitivity tests. Bottom: EDC δD record on the resulting ice chronologies: with $\delta^{18}\text{O}_{\text{atm}}$ age markers (blue) and without these age markers (orange).

240 The comparison of the EDC thinning function derived from the EDC3 and AICC2012 age scales shows variations of the same amplitude and at the same depths for the bottom part of the core (Fig. 7; Parrenin et al., 2007; Dreyfus et al., 2007). These variations also appear when only the $\delta\text{O}_2/\text{N}_2$ age markers are considered. This result is then common for the two types of orbital markers, giving us a good argument to assume that this behaviour is robust.

245 3.3 Δdepth markers

Δdepth markers are only given for NorthGRIP over the last glacial period. They have been obtained by a depth comparison of the $\delta^{18}\text{O}_{\text{ice}}$ and air $\delta^{15}\text{N}$ profiles over the succession of Dansgaard-Oeschger events. Because of thermal isotopic fractionation, each step in $\delta^{18}\text{O}_{\text{ice}}$ corresponding to a rapid warming is recorded as a peak in $\delta^{15}\text{N}$ in the gas phase. The Δdepth markers have been 250 measured as either the depth difference between the mid-slopes of $\delta^{18}\text{O}_{\text{ice}}$ and of $\delta^{15}\text{N}$ or as the depth difference between the peaks of $\delta^{18}\text{O}_{\text{ice}}$ and of $\delta^{15}\text{N}$. The uncertainty estimate is 2 m from the resolution of the measurements and the difference of Δdepth estimates (mid-slopes of peaks) (Table 3).

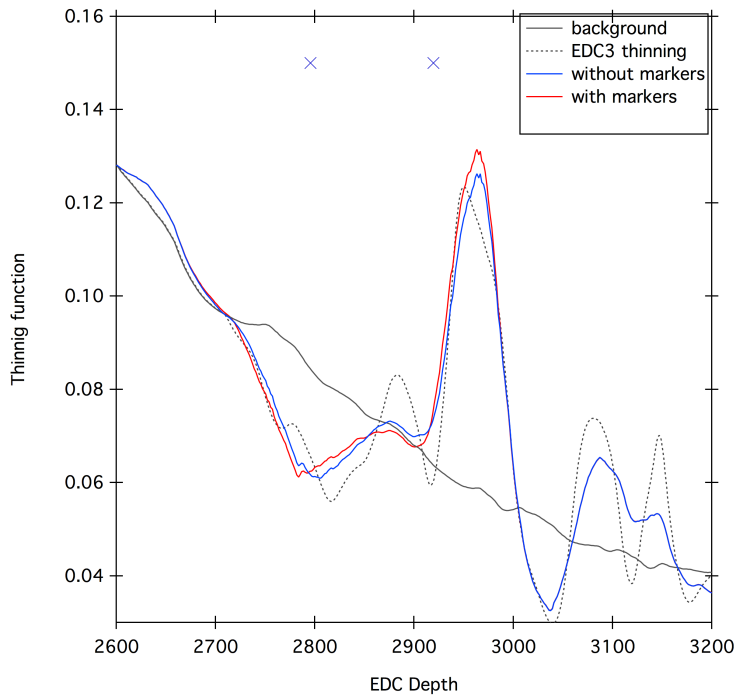


Fig. 7. Thinning function at EDC between 540-600 ka. Blue crosses mark the position of $\delta\text{O}_2/\text{N}_2$ age markers when accounted for (AICC2012, red curve) and without them (blue curve) cases.

3.4 Gas stratigraphic links

255 The gas stratigraphic links come from matching of CH_4 and $\delta^{18}\text{O}_{\text{atm}}$ variations between ice cores following the published tie-points (references are provided in Table 4 of gas stratigraphic tie-points). $\delta^{15}\text{N}$ data are used as markers of rapid warming in the NorthGRIP ice core when CH_4 data were not available (tie-points from Capron et al. (2010)). In some cases, the associated uncertainties had to be increased for obtaining the final chronology because of incoherencies in the final thinning,
260 accumulation rate or LIDIE scenarios. A few tie-points had also to be removed because of similar incoherencies.

3.5 Ice stratigraphic links

4 Application

Using all the previously cited inputs, the Datice tool is capable of calculating the best compromise
265 between the background ages and the observations, using an inverse method (Lemieux-Dudon et al., 2010). On Fig. 8 we can visualize the improvement of the EDC chronology in the 1200 to 1340 m depth range. The background chronologies are represented by the dashed-black curve for the gas age and dashed-grey curve for the ice age. Different observations are represented with their uncertainties:

Table 3. List of Δ depth markers for NGRIP included in Datice

| Depth(m) | Δ depth | Uncertainty (m) |
|----------|----------------|-----------------|
| 2099.9 | 16.29 | 2 |
| 2123.6 | 15.8 | 2 |
| 2157.1 | 15.56 | 2 |
| 2218.2 | 15.7 | 2 |
| 2255.6 | 12.85 | 2 |
| 2345.2 | 11.74 | 2 |
| 2364.5 | 12.36 | 2 |
| 2419.31 | 11.6 | 2 |
| 2465.1 | 8.85 | 2 |
| 2506.9 | 8.16 | 1.5 |
| 2577.8 | 7.66 | 1.5 |
| 2685.1 | 7.15 | 2 |
| 2890.2 | 5.54 | 2 |
| 2895.8 | 4.44 | 1.5 |
| 2936.5 | 7.8 | 1.5 |

Table 4. Gas stratigraphic links between ice cores

| Pairs | Nb. of points | Sources |
|----------------|---------------|---|
| Vostok-EDC | 67 | Lemieux-Dudon et al. (2010) |
| | | Loulergue (2007) |
| | | This study |
| Vostok-TALDICE | 8 | This study |
| Vostok-NGRIP | 5 | Landais et al. (2006) |
| EDC-EDML | 64 | Schilt et al. (2010) |
| | | Loulergue et al. (2007) |
| | | Loulergue (2007) |
| | | This study |
| EDC-TALDICE | 22 | Buiron et al. (2011) Schüpbach et al. (2011) |
| EDC-NGRIP | 6 | Schilt et al. (2010) |
| EDML-TALDICE | 13 | Schüpbach et al. (2011) |
| EDML-NGRIP | 45 | Lemieux-Dudon et al. (2010) |
| | | Schilt et al. (2010) |
| | | Capron et al. (2010) |
| NGRIP-TALDICE | 25 | Buiron et al. (2011) (revised NGRIP depth) |

Table 5. Ice stratigraphic links between ice cores

| Pairs | Nb. of points | Sources |
|-------------|---------------|--|
| Vostok-EDC | 104 | Udisti et al. (2004) Parrenin et al. (2012b) |
| EDC-EDML | 240 | Ruth et al. (2007) Severi et al. (2007) This study |
| EDC-TALDICE | 102 | Severi et al. (2012) |
| EDC-NGRIP | 2 | Louergue et al. (2007) |
| EDML-NGRIP | 86 | Vinther et al. (2013) Svensson et al. (2013) |

some gas stratigraphic links (blue squares), some ice stratigraphic links (red squares) and absolute
270 ice ages (yellow triangles). After applying the inverse method, we finally obtain the blue and red
curves corresponding to the best compromise between the background and observations for the gas
(blue) and ice (red) chronologies. For example, we can see that at 1200 m depth the previous gas age
was 80.5 ka (83.5 ka for the ice phase), now the new gas age is 81.5 ka (84.5 ka for the ice). Note that
the blue and red curves necessarily fit perfectly the ice and gas stratigraphic markers (red and blue
275 squares) because these stratigraphic markers are initially only given as depth constraints on each ice
core, their respective ages are then calculated on the new chronology. On Fig. 8, the stratigraphic
points have thus been placed corresponding to their calculated age on the new chronology. The error
bars stand for the initial age uncertainties associated with these stratigraphic links.

5 Uncertainty attached to the AICC2012 chronology

280 The calculation of the age uncertainty is done exactly the same way as in Lemieux-Dudon et al.
(2010) and presented in the main text of Bazin et al. (2013).
The error on the gas age is currently defined as the error on the ice age plus an error on the depth.
This overestimates the error when the stratigraphic links are provided on the gas phase (in this case,
the gas age uncertainty should be smaller than the ice age uncertainty). The two uncertainties are
285 close, with differences of only a few centuries. As a result, we have expressed the uncertainty for
each depth as the maximum between gas and ice uncertainty on the final AICC2012 chronology. An
exception was made for EDC over the last 60 ka because of the presence of many ice stratigraphic
markers between EDML and EDC. In this case, the ice age uncertainty should be much smaller than
the gas age uncertainty, mainly governed by uncertainty on the LIDIE determination. The high den-
290 sity of ice stratigraphic links with very small associated uncertainty (cf Table 5) means that the EDC
and EDML ice age uncertainties should be similar and equal to the EDML ice age uncertainty. We

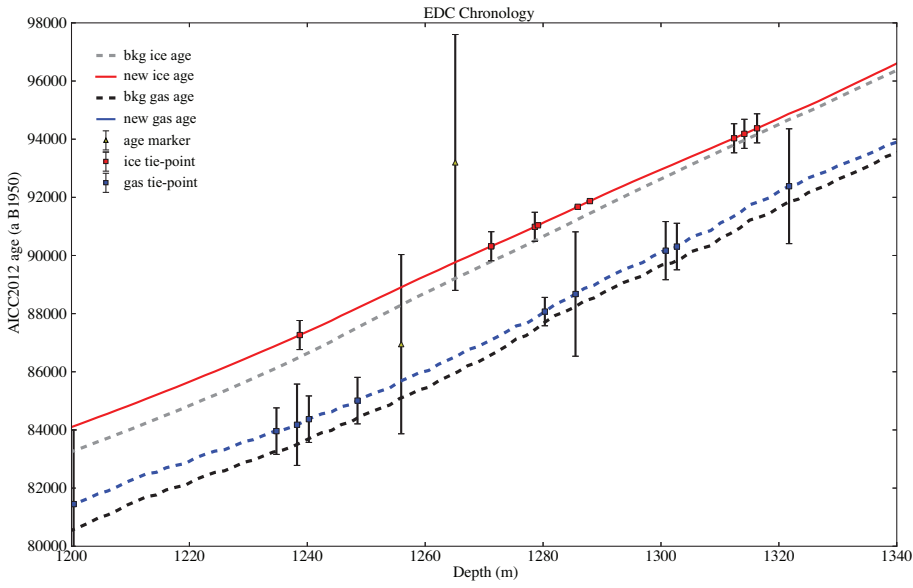


Fig. 8. Visualization of the Datice tool mechanism on the period 80 ka to 98 ka of the EDC ice core.

have thus assigned the values of EDML gas age uncertainty for the EDC ice age one over the last 60 ka. Moreover, the NGRIP uncertainty calculated by Datice for the last 60 ka has no meaning (not shown on Figure 10) as we have artificially constrained AICC2012 on GICC05 with age markers associated with small uncertainties (less than 50 years). As a result, the uncertainty of AICC2012 for NGRIP should be taken as the one of GICC05 (1 sigma = 1/2 MCE) over the last 60 ka.

Figure 9 shows the calculated error by DATICE (1 sigma) for the 5 ice cores on the AICC2012 chronology. As expected, the error increases with depth because of : (1) the increase of variance associated with background scenario, (2) less numerous absolute, orbital or stratigraphic constraints with depth, (3) the increase of uncertainties attached to data constraints with depth, and (4) the fact that error propagation applied to the ice age equation as a function of accumulation, and thinning cumulates the errors at each depth level. This is particularly visible for the NorthGRIP chronology where the numerous absolute tie-points over the last 60 ka are associated with an uncertainty of 1-50 years and much less data constraints prior to 60 ka. In presence of numerous age markers, the uncertainty of the chronology decreases as σ/\sqrt{N} , when N is the number of markers. For example, this explains why we observe an error of ~ 4 ka over a period constrained with several age markers of 6 ka uncertainty.

Focussing now on the last 60 ka, it is possible to explain the influence of the different inputs on the uncertainty of the final chronology (Fig. 10). In the absence of any absolute or stratigraphic tie-

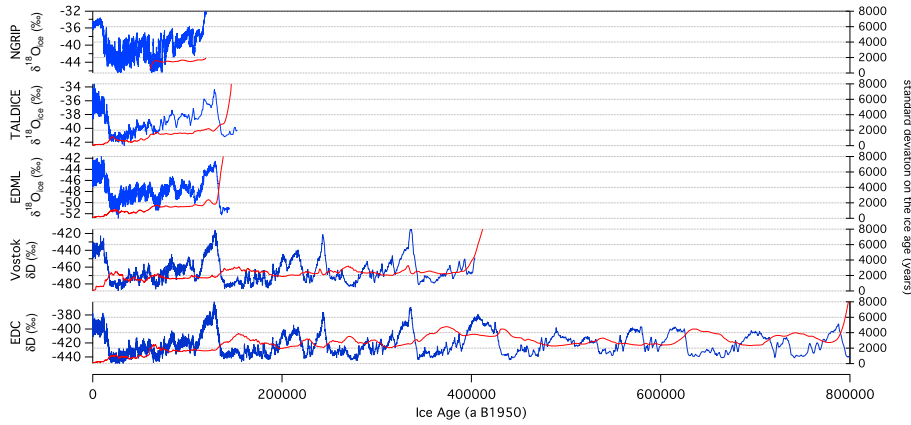


Fig. 9. $\delta^{18}\text{O}_{\text{ice}}$ records for the 5 ice cores on the AICC2012 chronology (blue) and standard deviation on ice ages for each ice core chronology (red).

points, the uncertainty will only be given by the variance associated with background scenario, hence much larger in the case of TALDICE than for EDC given our parameterization of variance (Table 2). Then, in the vicinity of stratigraphic or absolute tie-points, the uncertainty will be decreased
315 according to (1) the uncertainty of the tie-point itself and (2) the age uncertainty of the second ice core used in the case of stratigraphic tie-point. In Figure 10, we can separate different phases:

- From 0 to 11 ka, the main tie-points are volcanic ice stratigraphic tie-points. The uncertainty associated with these tie-points is small, as well as the uncertainty associated with thinning function and accumulation rate (close to present-day conditions and small depth). The smallest uncertainty for Antarctic ice cores is observed for EDML due to its stratigraphic links with NorthGRIP, whose chronology is given with a very small uncertainty (tuned to GICC05).
320
- Between 11–16 ka, we still have a few volcanic links but the chronology is mostly driven by methane links to the NorthGRIP ice core. Methane links are associated with larger uncertainties and with a more sparse resolution than volcanic tie-points. This leads to a general increase of the uncertainties of the Antarctic chronologies.
325
- The period 16–26 ka, roughly corresponding to MIS2, has the particularity of not being constrained with any marker for TALDICE. As a consequence, the final error is only function of the background variances, leading to an important increase of the chronology uncertainty especially for the TALDICE chronology that has the largest background variance for the thinning.
330
- Between 26 and 40 ka, the presence of (few) volcanic and (several) methane links, reduces the chronology uncertainty to the same level as during the last deglaciation.

335

- The Laschamp event is recorded as an absolute age marker on EDC and Vostok, and is reflected in the other ice cores through the volcanic and methane links. After the Laschamp event, we observe an increased uncertainty for all Antarctic ice core due to the loosening of constraints.

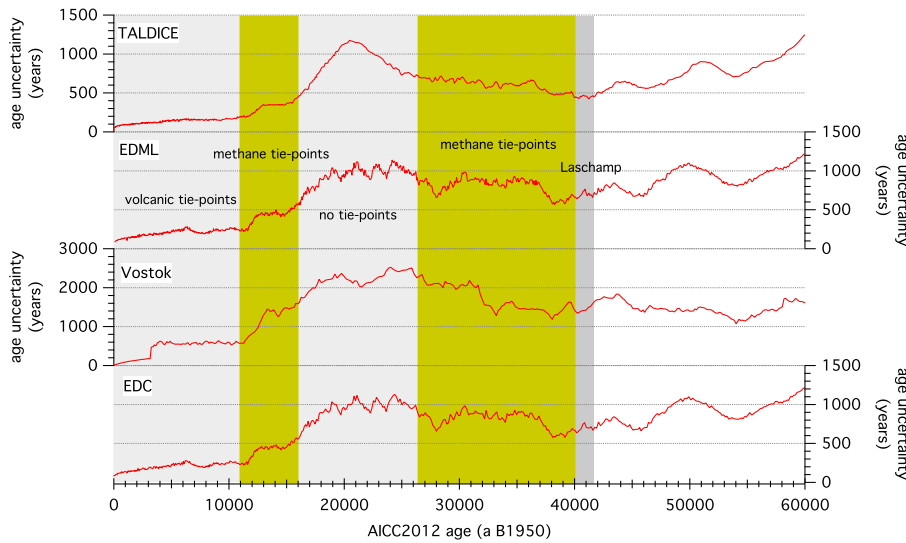


Fig. 10. AICC2012 uncertainty for TALDICE, EDML, Vostok and EDC over the last 60 ka.

6 Comparison with other chronologies

The comparison between EDC3 vs AICC2012 is discussed in the main text. Here we compare AICC2012 with other chronologies.

340 **6.1 AICC2012 vs Suwa and Bender (2008)**

Suwa and Bender (2008) have built a chronology for the Vostok ice core over the last 400 ka using $\delta\text{O}_2/\text{N}_2$ and $\delta^{18}\text{O}_{\text{atm}}$ orbital markers. Because the same markers are used in AICC2012, we expect some similarities between both chronologies. They are indeed very close: 3.5 ka max difference within the last glacial period due to the numerous stratigraphic links with other cores, otherwise less

345 than 2 ka difference over the last 400 ka (Fig. 11).

6.2 AICC2012 vs Kawamura et al. (2007)

Kawamura et al. (2007) have constructed the Dome F chronology back to 360 ka using $\delta\text{O}_2/\text{N}_2$ constraints (DFO-2006). AICC2012 appears consistent with the Dome F orbital chronology, within 2 ka, except for the last glacial inception (up to 5-6 ka difference with Dome F, and only 1.5 ka

350 difference with Suwa and Bender (2008), Fig. 11). This results from different relationships between
 $\delta\text{O}_2/\text{N}_2$ and δD records that are not really identical during MIS 5 at Dome F and Vostok. The
time difference between the AICC2012 timescale and Dome F DFO-2006 timescale is of the same
amplitude as the difference between DFO-2006 with the EDC3. To enhance the comparison, it
would be very interesting to compare also the AICC2012 gas chronology with Dome F gas age scale
355 using methane records when it will be published for Dome F.

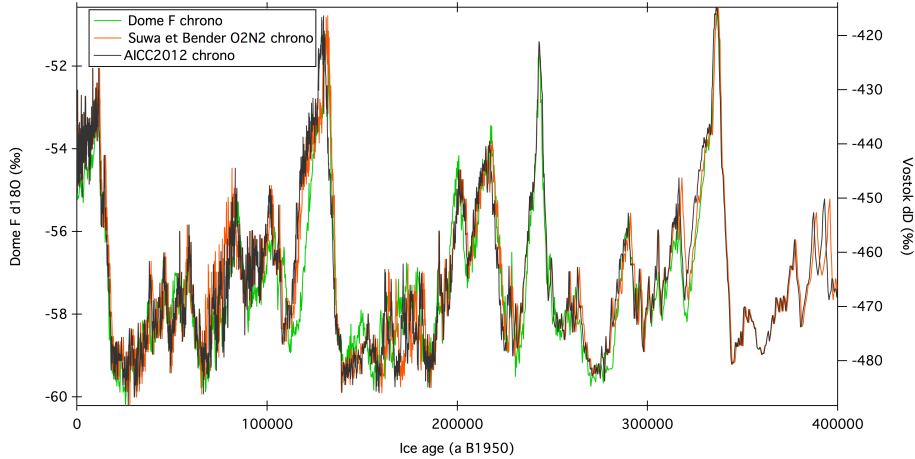


Fig. 11. Water isotopes of Dome F (green) and Vostok with different chronologies: Suwa et Bender 2008 (orange) and AICC2012 (black).

6.3 AICC2012 vs Parrenin et al. (2013) over the last deglaciation

Parrenin et al. (2013) have recently derived a new chronology for the EDC gas and ice records over the last deglaciation using $\delta^{15}\text{N}$ constraints for LIDIE determination at Dome C. We do not compare AICC2012 to Parrenin et al. (2013) in terms of absolute ages since this age scale was built only for
360 inferring the CO₂ / Antarctic temperature phasing. In term of relative phasing, AICC2012 confirms the findings of Parrenin et al. (2013), with no significant phase shift between CO₂ and Antarctic temperature at the onset of Termination I and Younger-Dryas and a small lag of CO₂ (slightly larger by 100-400 years in AICC2012) at the onset of Bølling-Allerød and Holocene.

6.4 AICC2012 vs speleothems

365 Following Fleitmann et al. (2009) who suggested that CH₄ abrupt variations over DO events and changes in speleothem $\delta^{18}\text{O}$ of calcite are in phase, we have compared some CH₄ abrupt transitions in AICC2012 with changes in Chinese speleothem records of calcite $\delta^{18}\text{O}$. This exercise has already been proposed to validate the Dome F chronology based on $\delta\text{O}_2/\text{N}_2$ measurements. The comparison is showed on Table 6. The AICC2012 chronology is in very good agreement with the speleothem

370 ages (within the uncertainty of the AICC2012 chronology; Cheng et al., 2009, 2012; Wang et al.,
2001, 2008), which give us confidence in the methodology used to construct this timescale.

Table 6. Comparison of AICC2012 with speleothems.

| Events | AICC2012 age (ka) | Speleothem age (ka) | |
|-------------|-------------------|---------------------|--------|
| DO-8 | 38.29 | MCL-Hulu | 38.32 |
| | | MSD-Hulu | 38.23 |
| DO-11 | 43.43 | MCL-Hulu | 43.81 |
| | | MSD-Hulu | 44.08 |
| DO-19 | 72.57 | MCL-Hulu | 72.17 |
| | | SB-22-Sanbao | 71.7 |
| DO-22 | 90.52 | SB25-1-Sanbao | 91.52 |
| | | SB22-Sanbao | 90.8 |
| onset MIS5 | 128.88 | SB25 | 129.04 |
| | | SB11 | 129.08 |
| onset MIS7 | 243.41 | B61 | 243.1 |
| | | LZ15 | 243.6 |
| onset MIS9 | 337.2 | B61 | 336.4 |
| | | LZ15 | 337.6 |
| onset MIS11 | 426.2 | Kesang | 426.6 |
| Onset MIS13 | 492.5 | Kesang | 492.1 |

References

- Andersen, K. K., Svensson, A., Johnsen, S. J., Rasmussen, S. O., Bigler, M., Röhlisberger, R., Ruth, U.,
375 Siggaard-Andersen, M.-L., Peder Steffensen, J., Dahl-Jensen, D., Vinther, B. M., and Clausen, H. B.: The
Greenland Ice Core Chronology 2005, 15–42 ka. Part 1: constructing the time scale, *Quaternary Science
Reviews*, 25, 3246–3257, doi:10.1016/j.quascirev.2006.08.002, 2006.
- Bazin, L., Landais, A., Lemieux-Dudon, B., Toyé Mahamadou Kele, H., Veres, D., Parrenin, F., Martinerie, P.,
Ritz, C., Capron, E., Lipenkov, V., Loutre, M.-F., Raynaud, D., Vinther, B., Svensson, A., Rasmussen, S.,
380 Severi, M., Blunier, T., Leuenberger, M., Fischer, H., Masson-Delmotte, V., Chappellaz, J., and Wolff, E.:
An optimized multi-proxies, multi-site Antarctic ice and gas orbital chronology (AICC2012): 120–800 ka,
Climate of the Past, This issue, 2013.
- Buiron, D., Chappellaz, J., Stenni, B., Frezzotti, M., Baumgartner, M., Capron, E., Landais, A., Lemieux-
Dudon, B., Masson-Delmotte, V., Montagnat, M., Parrenin, F., and Schilt, A.: TALDICE-1 age scale of the
385 Talos Dome deep ice core, East Antarctica, *Climate of the Past*, 7, 1–16, doi:10.5194/cp-7-1-2011, 2011.
- Camps, P., Singer, B. S., Carvallo, C., Goguitchaichvili, A., Fanjat, G., and Allen, B.: The Kamikatsura event
and the Matuyama-Brunhes reversal recorded in lavas from Tjörnes Peninsula, northern Iceland, *Earth and
Planetary Science Letters*, 310, 33–44, doi:10.1016/j.epsl.2011.07.026, 2011.
- Capron, E., Landais, A., Lemieux-Dudon, B., Schilt, A., Masson-Delmotte, V., Buiron, D., Chappellaz, J.,
390 Dahl-Jensen, D., Johnsen, S., Leuenberger, M., Louergue, L., and Oerter, H.: Synchronising EDML and
NorthGRIP ice cores using $\delta^{18}\text{O}$ of atmospheric oxygen ($\delta^{18}\text{O}_{\text{atm}}$) and CH_4 measurements over MIS5
(80–123 kyr), *Quaternary Science Reviews*, 29, 222–234, doi:10.1016/j.quascirev.2009.07.014, 2010.
- Capron, E., Landais, A., Buiron, D., Cauquoin, A., Chappellaz, J., Debret, M., Jouzel, J., Leuenberger, M.,
Martinerie, P., Masson-Delmotte, V., Mulvaney, R., Parrenin, F., and Prié, F.: Glacial-interglacial dynamics
395 of Antarctic firn: comparison between simulations and ice core air-d¹⁵N measurements, *Climate of the
Past*, 9, 983–999, doi:10.5194/cp-9-983-2013, 2013.
- Channell, J. E. T., Hodell, D. A., Singer, B. S., and Xuan, C.: Reconciling astrochronological and $^{40}\text{Ar}/^{39}\text{Ar}$
ages for the Matuyama-Brunhes boundary and late Matuyama Chron, *Geochemistry, Geophysics, Geosystems*, 11, Q0AA12, doi:10.1029/2010GC003203, 2010.
- 400 Cheng, H., Edwards, R. L., Broecker, W. S., Denton, G. H., Kong, X., Wang, Y., Zhang, R., and Wang, X.: Ice
Age Terminations, *Science*, 326, 248–252, doi:10.1126/science.1177840, 2009.
- Cheng, H., Zhang, P. Z., Spötl, C., Edwards, R. L., Cai, Y. J., Zhang, D. Z., Sang, W. C., Tan, M., and An,
Z. S.: The climatic cyclicity in semiarid-arid central Asia over the past 500,000 years, *Geophys. Res. Lett.*,
39, L01705, doi:10.1029/2011GL050202, 2012.
- 405 Dreyfus, G. B., Parrenin, F., Lemieux-Dudon, B., Durand, G., Masson-Delmotte, V., Jouzel, J., Barnola, J.-M.,
Panno, L., Spahni, R., Tisserand, A., Siegenthaler, U., and Leuenberger, M.: Anomalous flow below 2700
m in the EPICA Dome C ice core detected using $\delta^{18}\text{O}$ of atmospheric oxygen measurements, *Climate of the
Past*, 3, 341–353, doi:10.5194/cp-3-341-2007, 2007.
- Dreyfus, G. B., Raisbeck, G. M., Parrenin, F., Jouzel, J., Guyodo, Y., Nomade, S., and Mazaud, A.: An ice
410 core perspective on the age of the Matuyama-Brunhes boundary, *Earth and Planetary Science Letters*, 274,
151–156, doi:10.1016/j.epsl.2008.07.008, 2008.
- Dreyfus, G. B., Jouzel, J., Bender, M. L., Landais, A., Masson-Delmotte, V., and Leuenberger, M.: Firn pro-

- cesses and $\delta^{15}N$: potential for a gas-phase climate proxy, *Quaternary Science Reviews*, 29, 28 – 42, doi: 10.1016/j.quascirev.2009.10.012, 2010.
- 415 Dunbar, N. W., McIntosh, W. C., and Esser, R. P.: Physical setting and tephrochronology of the summit caldera ice record at Mount Moulton, West Antarctica, *Geological Society of America Bulletin*, 120, 796–812, doi: 10.1130/B26140.1, 2008.
- Fleitmann, D., Cheng, H., Badertscher, S., Edwards, R. L., Mudelsee, M., Göktürk, O. M., Fankhauser, A., Pickering, R., Raible, C. C., Matter, A., Kramers, J., and Tüysüz, O.: Timing and climatic impact of 420 Greenland interstadials recorded in stalagmites from northern Turkey, *Geophys. Res. Lett.*, 36, L19707, doi:10.1029/2009GL040050, 2009.
- Goujon, C., Barnola, J.-M., and Ritz, C.: Modeling the densification of polar firn including heat diffusion: Application to close-off characteristics and gas isotopic fractionation for Antarctica and Greenland sites, *Journal of Geophysical Research (Atmospheres)*, 108, 4792, doi:10.1029/2002JD003319, 2003.
- 425 Guillevic, M., Bazin, L., Landais, A., Masson- Delmotte, V., Blunier, T., Buchardt, S. L., Capron, E., Kindler, P., Leuenberger, M., Minster, B., Orsi, A., Prie, F., and Vinther, B. M.: Spatial gradients of temperature, accumulation and $\delta^{18}O$ -ice in Greenland over a series of Dansgaard-Oeschger events, *Climate of the Past*, 9, 1029–1051, doi:10.5194/cp-9-1029-2013, 2013.
- Huber, C., Beyerle, U., Leuenberger, M., Schwander, J., Kipfer, R., Spahni, R., Severinghaus, J. P., and Weiler, 430 K.: Evidence for molecular size dependent gas fractionation in firn air derived from noble gases, oxygen, and nitrogen measurements, *Earth and Planetary Science Letters*, 243, 61–73, doi:10.1016/j.epsl.2005.12.036, 2006.
- Huybrechts, P., Rybak, O., Pattyn, F., Ruth, U., and Steinhage, D.: Ice thinning, upstream advection, and non-climatic biases for the upper 89% of the EDML ice core from a nested model of the Antarctic ice sheet, 435 *Climate of the Past Discussions*, 3, 693–727, 2007.
- Kawamura, K., Parrenin, F., Lisiecki, L., Uemura, R., Vimeux, F., Severinghaus, J. P., Hutterli, M. A., Nakazawa, T., Aoki, S., Jouzel, J., Raymo, M. E., Matsumoto, K., Nakata, H., Motoyama, H., Fujita, S., Goto-Azuma, K., Fujii, Y., and Watanabe, O.: Northern Hemisphere forcing of climatic cycles in Antarctica over the past 360,000years, *Nature*, 448, 912–916, doi:10.1038/nature06015, 2007.
- 440 Kuiper, K. F., Deino, A., Hilgen, F. J., Krijgsman, W., Renne, P. R., and Wijbrans, J. R.: Synchronizing Rock Clocks of Earth History, *Science*, 320, 500–, doi:10.1126/science.1154339, 2008.
- Landais, A., Barnola, J. M., Masson-Delmotte, V., Jouzel, J., Chappellaz, J., Caillon, N., Huber, C., Leuenberger, M., and Johnsen, S. J.: A continuous record of temperature evolution over a sequence of Dansgaard-Oeschger events during Marine Isotopic Stage 4 (76 to 62 kyr BP), *Geophys. Res. Lett.*, 31, L22211, doi: 445 10.1029/2004GL021193, 2004.
- Landais, A., Jouzel, J., Massondelmotte, V., and Caillon, N.: Large temperature variations over rapid climatic events in Greenland: a method based on air isotopic measurements, *Comptes Rendus Geoscience*, 337, 947–956, doi:10.1016/j.crte.2005.04.003, 2005.
- Landais, A., Waelbroeck, C., and Masson-Delmotte, V.: On the limits of Antarctic and marine climate records 450 synchronization: Lag estimates during marine isotopic stages 5d and 5c, *Paleoceanography*, 21, PA1001, doi:10.1029/2005PA001171, 2006.
- Lemieux-Dudon, B., Blayo, E., Petit, J.-R., Waelbroeck, C., Svensson, A., Ritz, C., Barnola, J.-M., Narcisi,

- B. M., and Parrenin, F.: Consistent dating for Antarctic and Greenland ice cores, *Quaternary Science Reviews*, 29, 8–20, doi:10.1016/j.quascirev.2009.11.010, 2010.
- 455 Louergue, L.: Contraintes chronologiques et biogeochemiques grace au methane dans la glace naturelle : une application aux forages du projet EPICA, 2007, Ph.D. thesis, UJF, France, 2007.
- Louergue, L., Parrenin, F., Blunier, T., Barnola, J.-M., Spahni, R., Schilt, A., Raisbeck, G., and Chappellaz, J.: New constraints on the gas age-ice age difference along the EPICA ice cores, 0-50 kyr, *Climate of the Past*, 3, 527–540, 2007.
- 460 Mochizuki, N., Oda, H., Ishizuka, O., Yamazaki, T., and Tsunakawa, H.: Paleointensity variation across the Matuyama-Brunhes polarity transition: Observations from lavas at Punaruu Valley, Tahiti, *Journal of Geophysical Research (Solid Earth)*, 116, B06103, doi:10.1029/2010JB008093, 2011.
- Narcisi, B., Robert Petit, J., and Tiepolo, M.: A volcanic marker (92 ka) for dating deep east Antarctic ice cores, *Quaternary Science Reviews*, 25, 2682–2687, doi:10.1016/j.quascirev.2006.07.009, 2006.
- 465 NorthGRIP Community Members: High-resolution record of Northern Hemisphere climate extending into the last interglacial period, *Nature*, 431, 147–151, doi:10.1038/nature02805, 2004.
- Parrenin, F., Jouzel, J., Waelbroeck, C., Ritz, C., and Barnola, J.-M.: Dating the Vostok ice core by an inverse method, *J. Geophys. Res.*, 106, 31 837–31 852, doi:10.1029/2001JD900245, 2001.
- 470 Parrenin, F., Barnola, J.-M., Beer, J., Blunier, T., Castellano, E., Chappellaz, J., Dreyfus, G., Fischer, H., Fujita, S., Jouzel, J., Kawamura, K., Lemieux-Dudon, B., Louergue, L., Masson-Delmotte, V., Narcisi, B., Petit, J.-R., Raisbeck, G., Raynaud, D., Ruth, U., Schwander, J., Severi, M., Spahni, R., Steffensen, J. P., Svensson, A., Udisti, R., Waelbroeck, C., and Wolff, E.: The EDC3 chronology for the EPICA Dome C ice core, *Climate of the Past*, 3, 485–497, doi:10.5194/cp-3-485-2007, 2007.
- 475 Parrenin, F., Barker, S., Blunier, T., Chappellaz, J., Jouzel, J., Landais, A., Masson-Delmotte, V., Schwander, J., and Veres, D.: On the gas-ice depth difference (Δ depth) along the EPICA Dome C ice core, *Climate of the Past Discussions*, 8, 1089–1131, doi:10.5194/cpd-8-1089-2012, 2012a.
- Parrenin, F., Petit, J.-R., Masson-Delmotte, V., Wolff, E., Basile-Doelsch, I., Jouzel, J., Lipenkov, V., Rasmussen, S. O., Schwander, J., Severi, M., Udisti, R., Veres, D., and Vinther, B. M.: Volcanic synchronisation between the EPICA Dome C and Vostok ice cores (Antarctica) 0-145 kyr BP, *Climate of the Past*, 8, 1031–1045, doi:10.5194/cp-8-1031-2012, 2012b.
- 480 Parrenin, F., Masson-Delmotte, V., Khler, P., Raynaud, D., Paillard, D., Schwander, J., Barbante, C., Landais, A., Wegner, A., and Jouzel, J.: Synchronous Change of Atmospheric CO₂ and Antarctic Temperature During the Last Deglacial Warming, *Science*, 339, 1060–1063, doi:10.1126/science.1226368, 2013.
- Raisbeck, G., Yiou, F., Bard, E., Dollfus, D., Jouzel, J., and Petit, J. R.: Absolute dating of the last 7000 years of the Vostok ice core using ^{10}Be , *Mineral. Mag.*, 62A, 1228, 1998.
- 485 Raisbeck, G. M., Yiou, F., Bourles, D., Lorius, C., and Jouzel, J.: Evidence for two intervals of enhanced Be-10 deposition in Antarctic ice during the last glacial period, *Nature*, 326, 273–277, doi:10.1038/326273a0, 1987.
- Raisbeck, G. M., Yiou, F., Cattani, O., and Jouzel, J.: ^{10}Be evidence for the Matuyama-Brunhes geomagnetic reversal in the EPICA Dome C ice core, *Nature*, 444, 82–84, doi:10.1038/nature05266, 2006.
- 490 Rasmussen, S. O., Andersen, K. K., Svensson, A. M., Steffensen, J. P., Vinther, B. M., Clausen, H. B., Siggaard-Andersen, M.-L., Johnsen, S. J., Larsen, L. B., Dahl-Jensen, D., Bigler, M., Röhlisberger, R., Fischer, H.,

- Goto-Azuma, K., Hansson, M. E., and Ruth, U.: A new Greenland ice core chronology for the last glacial termination, *Journal of Geophysical Research (Atmospheres)*, 111, D06102, doi:10.1029/2005JD006079, 495 2006.
- Renne, P. R., Swisher, C. C., Deino, A. L., Karner, D. B., Owens, T. L., and DePaolo, D. J.: Intercalibration of standards, absolute ages and uncertainties in $^{40}\text{Ar}/^{39}\text{Ar}$ dating, *Chemical Geology*, 145, 117 – 152, doi: 10.1016/S0009-2541(97)00159-9, 1998.
- Ruth, U., Barnola, J.-M., Beer, J., Bigler, M., Blunier, T., Castellano, E., Fischer, H., Fundel, F., Huybrechts, 500 P., Kaufmann, P., Kipfstuhl, S., Lambrecht, A., Morganti, A., Oerter, H., Parrenin, F., Rybak, O., Severi, M., Udisti, R., Wilhelms, F., and Wolff, E.: "EDML1": a chronology for the EPICA deep ice core from Dronning Maud Land, Antarctica, over the last 150 000 years, *Climate of the Past*, 3, 475–484, doi:10.5194/cp-3-475-2007, 2007.
- Schilt, A., Baumgartner, M., Blunier, T., Schwander, J., Spahni, R., Fischer, H., and Stocker, T. F.: Glacial-interglacial and millennial-scale variations in the atmospheric nitrous oxide concentration during the last 505 800,000 years, *Quaternary Science Reviews*, 29, 182–192, doi:10.1016/j.quascirev.2009.03.011, 2010.
- Schüpbach, S., Federer, U., Bigler, M., Fischer, H., and Stocker, T. F.: A refined TALDICE-1a age scale from 55 to 112 ka before present for the Talos Dome ice core based on high-resolution methane measurements, *Climate of the Past*, 7, 1001–1009, doi:10.5194/cp-7-1001-2011, 2011.
- 510 Severi, M., Becagli, S., Castellano, E., Morganti, A., Traversi, R., Udisti, R., Ruth, U., Fischer, H., Huybrechts, P., Wolff, E., Parrenin, F., Kaufmann, P., Lambert, F., and Steffensen, J. P.: Synchronisation of the EDML and EDC ice cores for the last 52 kyr by volcanic signature matching, *Climate of the Past*, 3, 367–374, 2007.
- Severi, M., Udisti, R., Becagli, S., Stenni, B., and Traversi, R.: Volcanic synchronisation of the EPICA-DC and 515 TALDICE ice cores for the last 42 kyr BP, *Climate of the Past*, 8, 509–517, doi:10.5194/cp-8-509-2012, 2012.
- Singer, B. S., Guillou, H., Jicha, B. R., Laj, C., Kissel, C., Beard, B. L., and Johnson, C. M.: $^{40}\text{Ar}/^{39}\text{Ar}$, K-Ar and $^{230}\text{Th}-^{238}\text{U}$ dating of the Laschamp excursion: A radioisotopic tie-point for ice core and climate chronologies, *Earth and Planetary Science Letters*, 286, 80–88, doi:10.1016/j.epsl.2009.06.030, 2009.
- Sowers, T., Bender, M., Raynaud, D., and Korotkevich, Y. S.: $\delta^{15}\text{N}$ of N_2 in Air Trapped in Polar Ice: a Tracer 520 of Gas Transport in the Firn and a Possible Constraint on Ice Age-Gas Age Differences, *J. Geophys. Res.*, 97, 15 683–15 697, doi:10.1029/92JD01297, 1992.
- Suwa, M. and Bender, M. L.: Chronology of the Vostok ice core constrained by O_2/N_2 ratios of occluded air, and its implication for the Vostok climate records, *Quaternary Science Reviews*, 27, 1093–1106, doi: 10.1016/j.quascirev.2008.02.017, 2008.
- 525 Svensson, A., Andersen, K. K., Bigler, M., Clausen, H. B., Dahl-Jensen, D., Davies, S. M., Johnsen, S. J., Muscheler, R., Parrenin, F., Rasmussen, S. O., Röhlisberger, R., Seierstad, I., Steffensen, J. P., and Vinther, B. M.: A 60 000 year Greenland stratigraphic ice core chronology, *Climate of the Past*, 4, 47–57, doi: 10.5194/cp-4-47-2008, 2008.
- Svensson, A., Bigler, M., Blunier, T., Clausen, H. B., Dahl-Jensen, D., Fischer, H., Fujita, S., Goto-Azuma, K., 530 Johnsen, S. J., Kawamura, K., Kipfstuhl, S., Kohno, M., Parrenin, F., Popp, T., Rasmussen, S. O., Schwander, J., Seierstad, I., Severi, M., Steffensen, J. P., Udisti, R., Uemura, R., Vallelonga, P., Vinther, B. M., Wegner, A., Wilhelms, F., and Winstrup, M.: Direct linking of Greenland and Antarctic ice cores at the Toba eruption

- (74 ka BP), *Climate of the Past*, 9, 749–766, doi:10.5194/cp-9-749-2013, 2013.
- Udisti, R., Becagli, S., Castellano, E., Delmonte, B., Jouzel, J., Petit, J. R., Schwander, J., Stenni, B., and Wolff, E. W.: Stratigraphic correlations between the European Project for Ice Coring in Antarctica (EPICA) Dome C and Vostok ice cores showing the relative variations of snow accumulation over the past 45 kyr, *Journal of Geophysical Research (Atmospheres)*, 109, D08101, doi:10.1029/2003JD004180, 2004.
- Veres, D., Bazin, L., Landais, A., Lemieux-Dudon, B., Parrenin, F., Martinerie, P., Toyé Mahamadou Kele, H., Capron, E., Chappellaz, J., Rasmussen, S., Severi, M., Svensson, A., Vinther, B., and Wolff, E.: The Antarctic ice core chronology (AICC2012): an optimized multi-parameter and multi-site dating approach for the last 120 thousand years, *Climate of the Past*, This issue, 2013.
- Vinther, B., Clausen, H., Kipfstuhl, S., Fischer, H., Bigler, M., Oerter, H., Wegner, A., Wilhelms, F., Sevri, M., Udisti, R., Beer, J., Steinhilber, F., Adolphi, F., Muschler, R., Rasmussen, S., Steffensen, J., and Svensson, A.: A stratigraphic Antarctic chronology covering the past 16700 years in the EPICA deep ice core from Dronning Maud Land, In prep, 2013.
- Vinther, B. M., Clausen, H. B., Johnsen, S. J., Rasmussen, S. O., Andersen, K. K., Buchardt, S. L., Dahl-Jensen, D., Seierstad, I. K., Siggaard-Andersen, M.-L., Steffensen, J. P., Svensson, A., Olsen, J., and Heinemeier, J.: A synchronized dating of three Greenland ice cores throughout the Holocene, *Journal of Geophysical Research (Atmospheres)*, 111, D13102, doi:10.1029/2005JD006921, 2006.
- Waelbroeck, C., Frank, N., Jouzel, J., Parrenin, F., Masson-Delmotte, V., and Genty, D.: Transferring radiometric dating of the last interglacial sea level high stand to marine and ice core records, *Earth and Planetary Science Letters*, 265, 183–194, doi:10.1016/j.epsl.2007.10.006, 2008.
- Wang, Y., Cheng, H., Edwards, R. L., Kong, X., Shao, X., Chen, S., Wu, J., Jiang, X., Wang, X., and An, Z.: Millennial- and orbital-scale changes in the East Asian monsoon over the past 224,000 years, *Nature*, 451, 1090–1093, doi:10.1038/nature06692, 2008.
- Wang, Y. J., Cheng, H., Edwards, R. L., An, Z. S., Wu, J. Y., Shen, C.-C., and Dorale, J. A.: A High-Resolution Absolute-Dated Late Pleistocene Monsoon Record from Hulu Cave, China, *Science*, 294, 2345–2348, doi:10.1126/science.1064618, 2001.
- Wolff, E. W., Chappellaz, J., Blunier, T., Rasmussen, S. O., and Svensson, A.: Millennial-scale variability during the last glacial: The ice core record, *Quaternary Science Reviews*, 29, 2828–2838, doi:10.1016/j.quascirev.2009.10.013, 2010.
- Yiou, F., Raisbeck, G. M., Baumgartner, S., Beer, J., Hammer, C., Johnsen, S., Jouzel, J., Kubik, P. W., Lestringuez, J., Stiévenard, M., Suter, M., and Yiou, P.: Beryllium 10 in the Greenland Ice Core Project ice core at Summit, Greenland, *J. Geophys. Res.*, 102, 26 783–26 794, doi:10.1029/97JC01265, 1997.